



Beta-induced Alfvén eigenmodes and geodesic acoustic modes in the presence of strong tearing activity during the current ramp-down on JET

Plasma Phys. Control. Fusion **9** (2022)

G. Pucella, E. Alessi, F. Auriemma, P. Buratti, M.V. Falessi, E. Giovannozzi, F. Zonca, M. Baruzzo, C.D. Challis, R. Dumont, D. Frigione, L. Garzotti, J. Hobirk, A. Kappatou, D.L. Keeling, D. King, V.G. Kiptily, E. Lerche, P.J. Lomas, M. Maslov, I. Nunes, F. Rimini, P. Sirén, C. Sozzi, M.F. Stamp, Z. Stancar, H. Sun, D. Van Eester, M. Zerbini, and JET Contributors



This work has been carried out within the framework of the EUROfusion Consortium and has received funding from the Euratom research and training programme 2014-2018 and 2019-2020 under grant agreement No 633053. The views and opinions expressed herein do not necessarily reflect those of the European Commission.



● **Experimental observations and theoretical framework**

- Additional magnetic oscillations in pulses with large magnetic islands
- Modes in the low-frequency range of the Alfvén continuum

● **Low frequency modes in early landing phase**

- Tearing mode activity and additional oscillations with $n = \pm 1$
- Coupled Alfvén-acoustic continuum by FALCON code
- Excitation of additional modes with $n = \pm 2$
- Dependency on plasma parameters
- Threshold on the magnetic island width

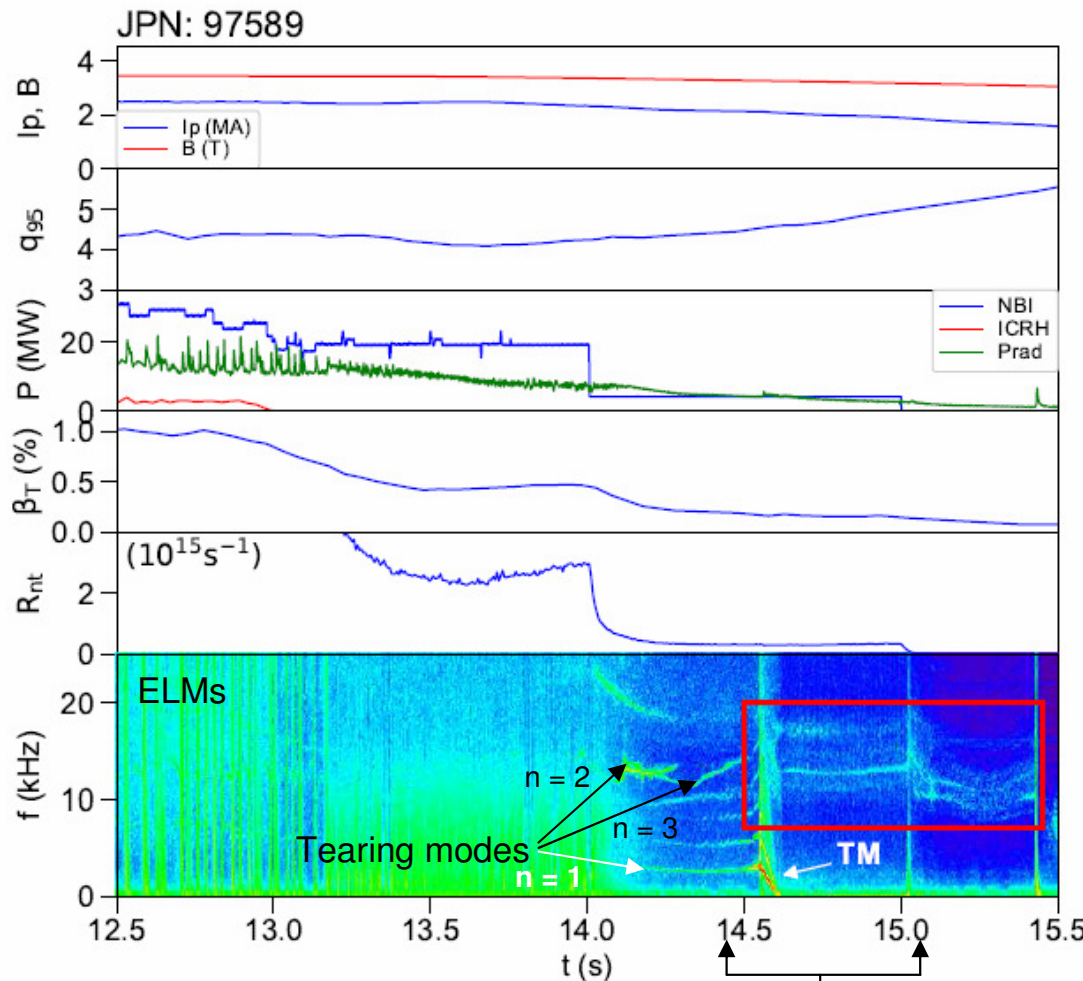
● **Non-linear mode coupling in late landing phase**

- Observation of multiple “triplets” (“twin BAEs” plus GAM) with slowly-rotating TM
- Cross-spectral coherence and bicoherence analysis

Experimental observations

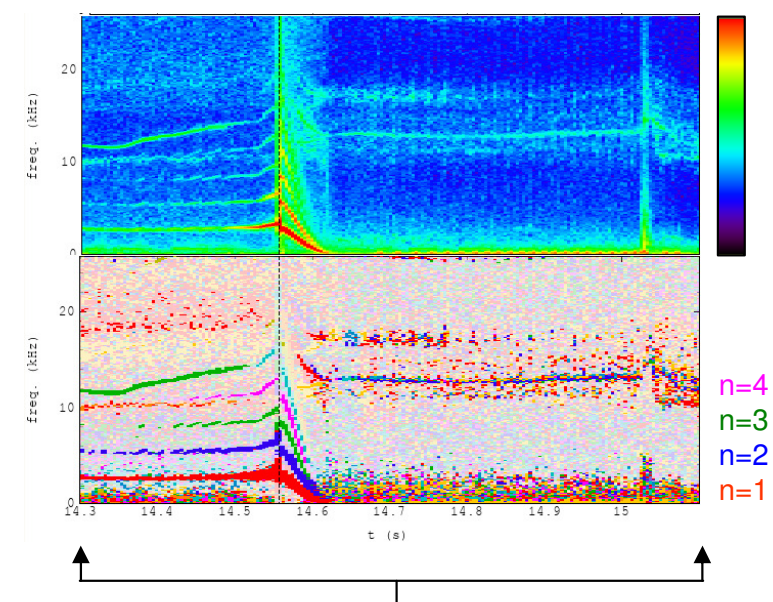


- The analysis of the current ramp-down phase of JET plasmas has revealed the occurrence of additional magnetic oscillations (**5-20 kHz**) in pulses characterized by large magnetic islands.



- Large dataset of pulses (600) analyzed. Final selection of 55 pulses:

- magnetic islands remaining at large amplitude for a relatively long time
- plasma rotating phases



Theoretical framework

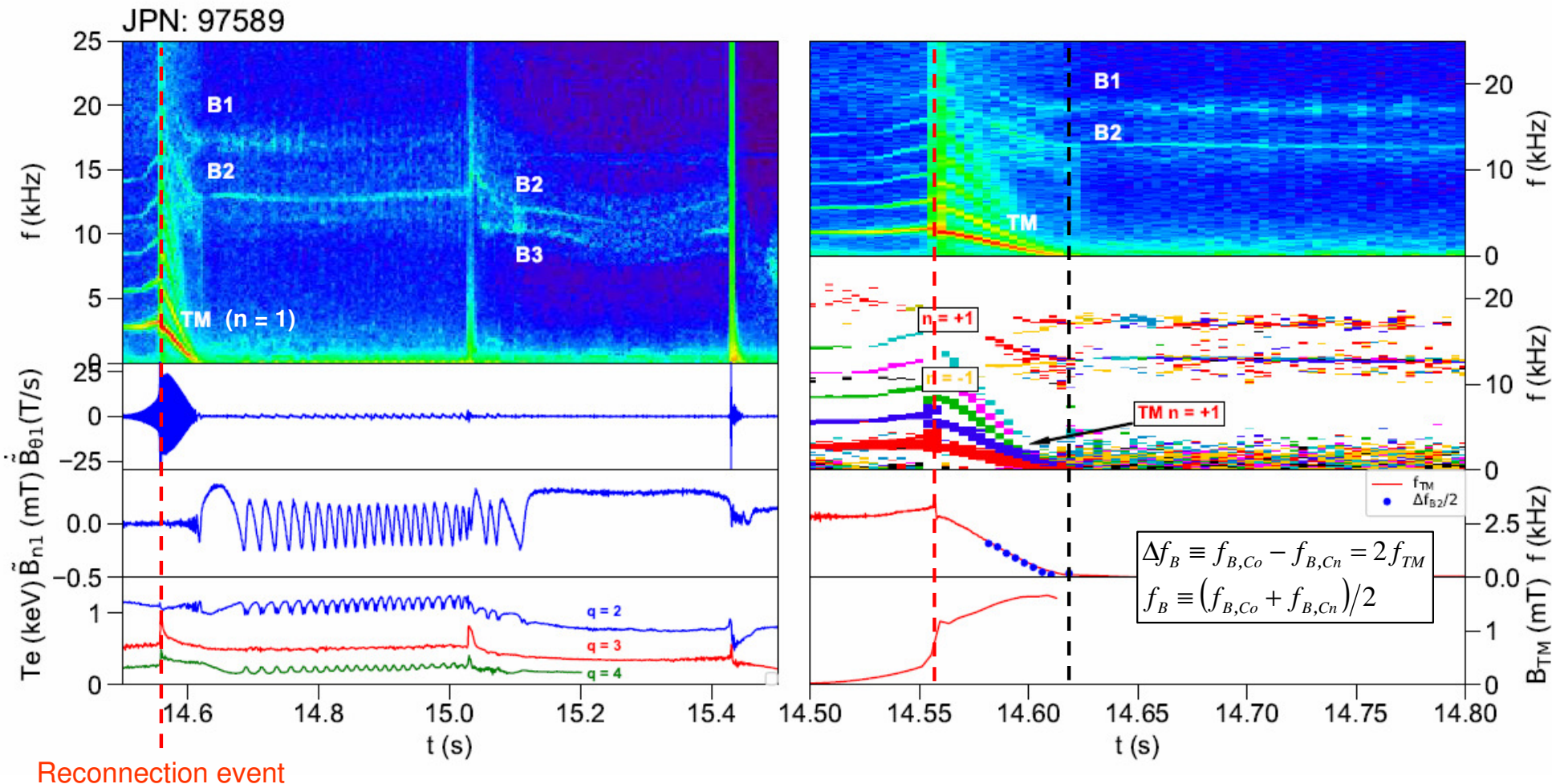


- The frequencies of the additional oscillations ($\omega \sim 0.1 \omega_A$) are well below the gaps in the Alfvén continuum due to ellipticity (EAE, $\omega \sim \omega_A$) or toroidicity (TAE, $\omega \sim \omega_A/2$), and of the same order as the gaps opened by plasma compressibility.
- **Beta-induced Alfvén eigenmodes** (BAE) are shear Alfvén waves falling in the low-frequency gap opened by plasma compressibility, which enters through the geodesic curvature and the finite β effect
 - Plasmas with energetic particles (DIII-D, TFTR, Tore-Supra, KSTAR, EAST)
 - Plasmas without any fast particle populations during strong tearing activity (FTU, TEXTOR, HL-2A, J-TEXT).
- **Geodesic acoustic modes** (GAM) are a kind of zonal flow with finite real frequency owing to the geodesic curvature of a toroidal magnetic field, driven by microscopic turbulence and supported by plasma compressibility in toroidal geometry.
 - Non-linear interaction between GAM, TM and BAE firstly observed in HL-2A and recently on EAST
- **Beta-induced Alfvén-acoustic eigenmodes** (BAAE) are waves with mixed polarization located in the gaps of the coupled Alfvén-acoustic continuum.
 - Instabilities identified as BAAE have been observed on JET, NSTX, DIII-D and HL-2A (driven by fast ions)
- Kinetic ballooning modes (KBM), Alfvén ion temperature gradient modes (AITG), ...
- The hypothesis we would like to support is that the additional oscillations sometimes observed in pulses with **strong tearing activity** are **BAE** (and **GAM**).

Low-frequency modes in the early landing phase



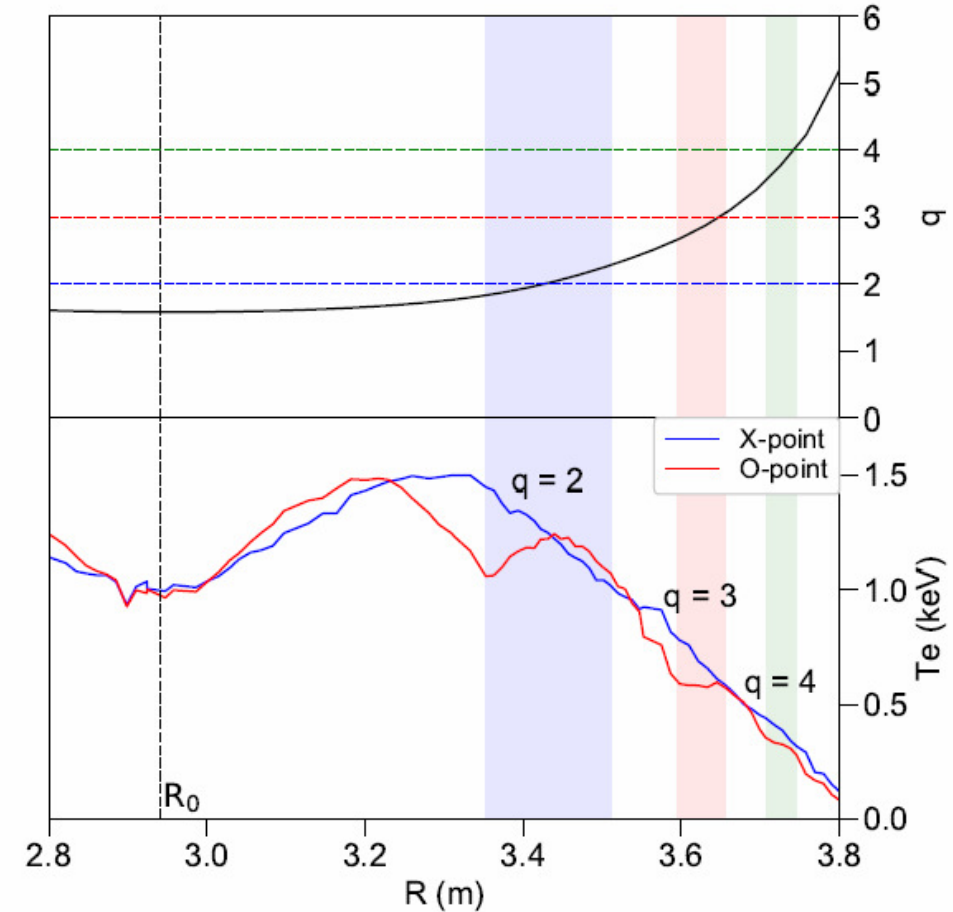
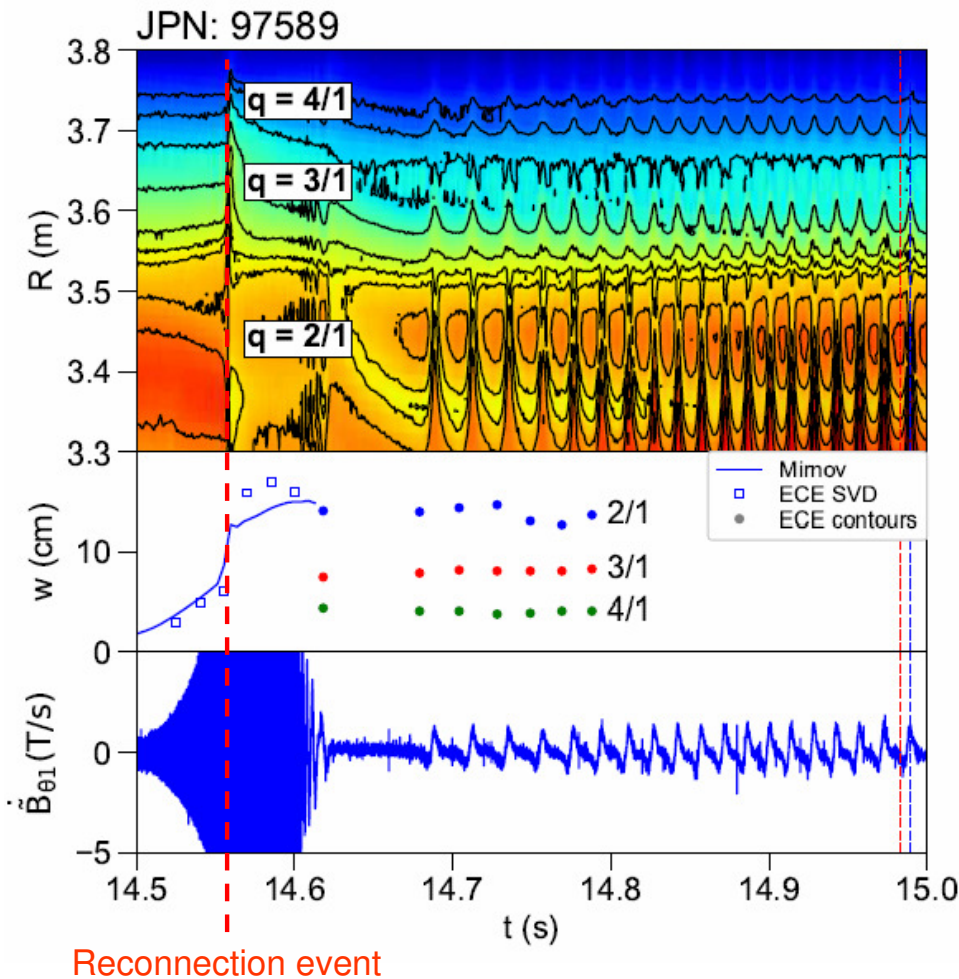
- $n = 1$ tearing activity in a pulse with hollow Te profile (linear destabilization).
- Multiple oscillations (B1, B2 and B3) between **5 and 20 kHz** after the transition to higher TM amplitudes, supporting the hypothesis of a threshold effect on TM amplitude for the excitation of the additional oscillations by a non-linear coupling mechanism [Buratti 2005, Chen 2011, Liu 2015].



Low-frequency modes in the early landing phase



- Time traces of ECE contours highlight the simultaneous presence of magnetic islands rotating with the same toroidal velocity at three different locations, which are in agreement with the position of the resonant surfaces corresponding to $q = 2$, $q = 3$ and $q = 4$, as estimated by the equilibrium safety factor profile.
- Hypothesis: components B1, B2 and B3 are pairs of BAEs associated with different magnetic islands.



Frequency range and scaling with temperature



- Ideal MHD predicts the frequency of the BAE to be located in the gap [Turnbull 1993]:

$$0 < \omega^2 < \gamma q^2 \beta \omega_A^2 \approx \gamma q^2 (1 + \tau) \omega_{ti}^2$$

$$v_A = B / \sqrt{4\pi\rho} ; \quad \omega_A = v_A / qR_0 ; \quad \omega_{ti} = \sqrt{2T_i/m_i} / qR_0 ; \quad \beta = 8\pi p / B^2 ; \quad \tau \equiv T_e / T_i$$

- Fluid limit of the kinetic theory of low-frequency Alfvén modes [Zonca 1996]:

$$\omega_{CAP}^2 = \frac{1}{R_0} \left(\frac{7}{4} + \frac{T_e}{T_i} \right) \frac{2T_i}{m_i} = q^2 \left(\frac{7}{4} + \tau \right) \omega_{ti}^2 \quad \rightarrow \quad \gamma = \frac{7/4 + \tau}{1 + \tau} \quad \text{effective polytropic index}$$

Continuum Accumulation Point

JPN: 97589

$$t = 14.7 \text{ s} : \quad \begin{cases} R_0 = 2.93 \text{ m} \\ T_i \approx T_e \end{cases} \quad \rightarrow \quad f_{CAP} (\text{kHz}) \approx 27 \sqrt{T_e (\text{keV})}$$

island 2/1 \Leftrightarrow BAEs B1	
$f_{CAP,2/1} \approx 27 \text{ kHz}$	$f_{B1} \approx 17 \text{ kHz}$
island 3/1 \Leftrightarrow BAEs B2	
$f_{CAP,3/1} \approx 19 \text{ kHz}$	$f_{B2} \approx 13 \text{ kHz}$
island 4/1 \Leftrightarrow BAEs B3	
$f_{CAP,4/1} \approx 13 \text{ kHz}$	$f_{B3} \approx 11 \text{ kHz}$

- BAE associated with different magnetic islands, with frequency values related to the temperature on the respective resonant surfaces.
- Shear Alfvén continuum by FALCON code in toroidal geometry [Falessi 2019] →

SAW-ISW continuum in the ideal MHD limit



- **Shear-Alfvén wave** (SAW) and **ion sound wave** (ISW) continuous frequency spectra are coupled due to equilibrium magnetic field curvature.

- Radial singular structures corresponding to the continuous spectra are obtained from the limiting forms ($|\vartheta| \rightarrow \infty$) of vorticity and pressure equations:

$$\begin{cases} \left(\partial_\eta^2 + \hat{\rho}_{m0} \hat{J}_\eta^2 \Omega^2 \right) g_1 = \left(2 \hat{B}_0 \hat{\rho}_{m0}^{1/2} \hat{J}_\eta^2 \hat{\kappa}_g \Omega \right) g_2 \\ \left(\partial_\eta^2 - |\nabla r| \partial_\eta^2 |\nabla r|^{-1} + \frac{2}{\Gamma \beta} \hat{\rho}_{m0} \hat{J}_\eta^2 \Omega^2 \right) g_2 = \left(2 \hat{B}_0 \hat{\rho}_{m0}^{1/2} \hat{J}_\eta^2 \hat{\kappa}_g \Omega \right) g_1 \end{cases}$$

$$\begin{cases} g_1 : \text{Alfvénic} \\ g_2 : \text{acoustic} \\ \Omega = \omega R_0 / \bar{v}_{A0} \\ \hat{\kappa}_g = \kappa_g R_0 \\ \kappa_g : \text{geodesic curvature} \end{cases}$$

- Slow-sound approximation:

$$\frac{\hat{\rho}_{m0}}{\Gamma \beta} \gg 1 \Rightarrow \left(\partial_\eta^2 + \hat{\rho}_{m0} \hat{J}_\eta^2 \Omega^2 - 2 \Gamma \beta \hat{J}_\eta^2 \hat{B}_0^2 \hat{\kappa}_g^2 \right) g_1 = 0$$

- Incompressible ideal MHD limit:

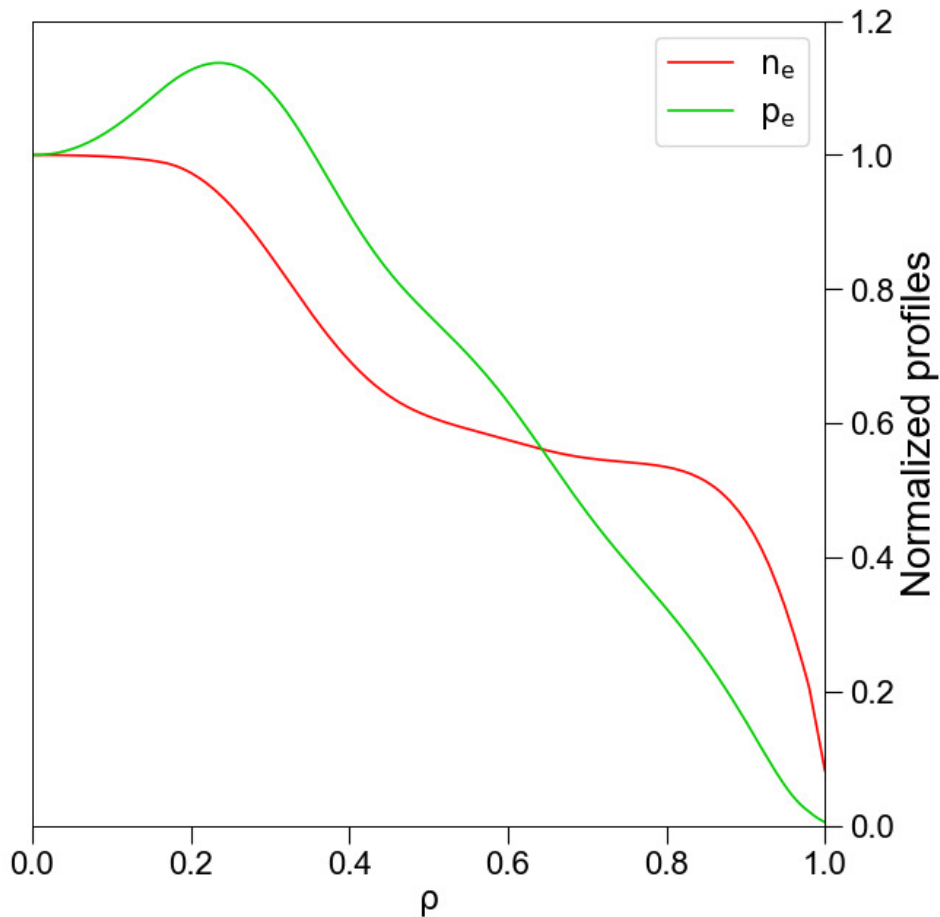
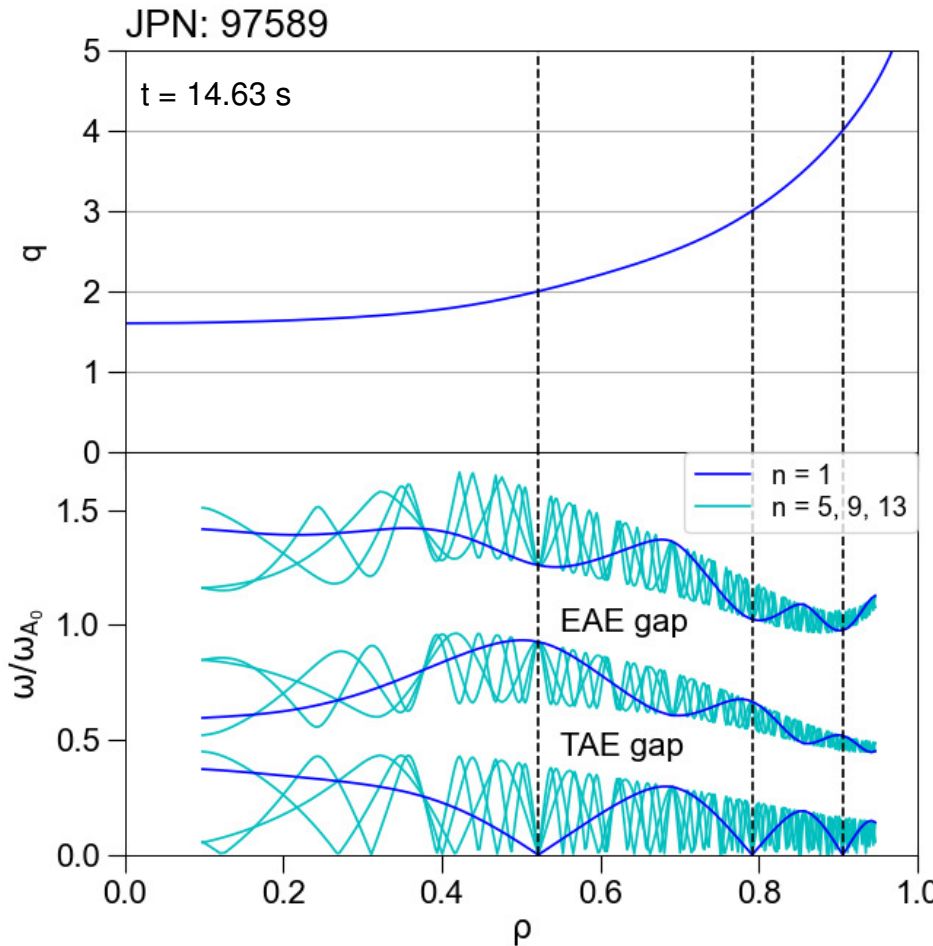
$$\frac{\hat{\rho}_{m0}}{\Gamma \beta} \rightarrow \infty \Rightarrow \left(\partial_\eta^2 + \hat{\rho}_{m0} \hat{J}_\eta^2 \Omega^2 \right) g_1 = 0$$

Incompressible ideal MHD limit



- SAW continuous spectrum calculated by FALCON code in the incompressible limit starting from the reconstructed equilibrium in the realistic toroidal geometry for JPN 97589.
- Ellipticity- and toroidicity-induced frequency gaps at $\omega \sim \omega_A$ (**EAE**) and $\omega \sim \omega_A/2$ (**TAE**), respectively.

$$\omega_{A0} = v_{A0}/q_0 R_0$$



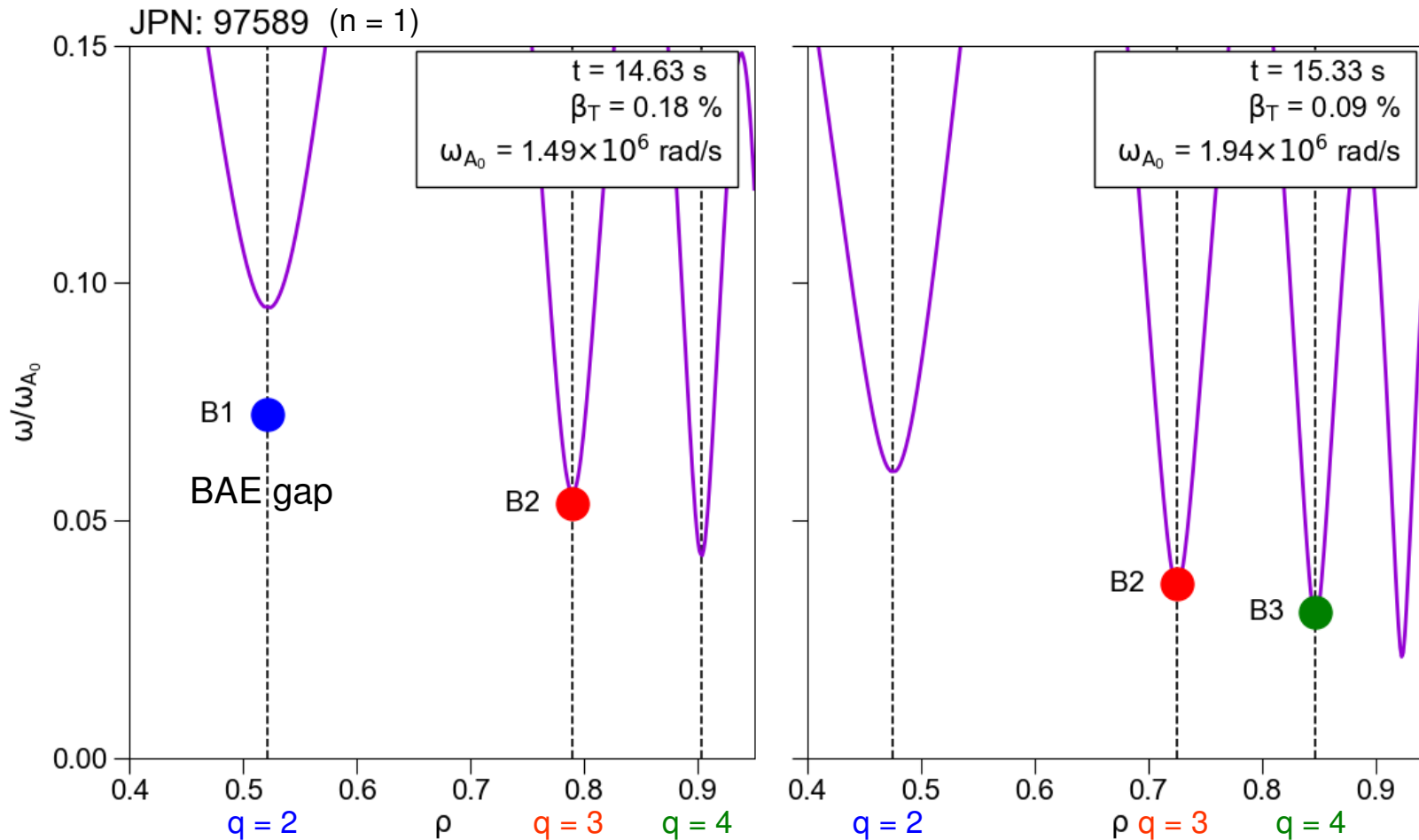
Slow-sound approximation



- Slow-sound approximation (violet line) with ideal MHD results re-scaled to account for kinetic effects:

$$\gamma = (7/4 + \tau)/(1 + \tau) \quad ; \quad \tau \equiv T_e/T_i = 1$$

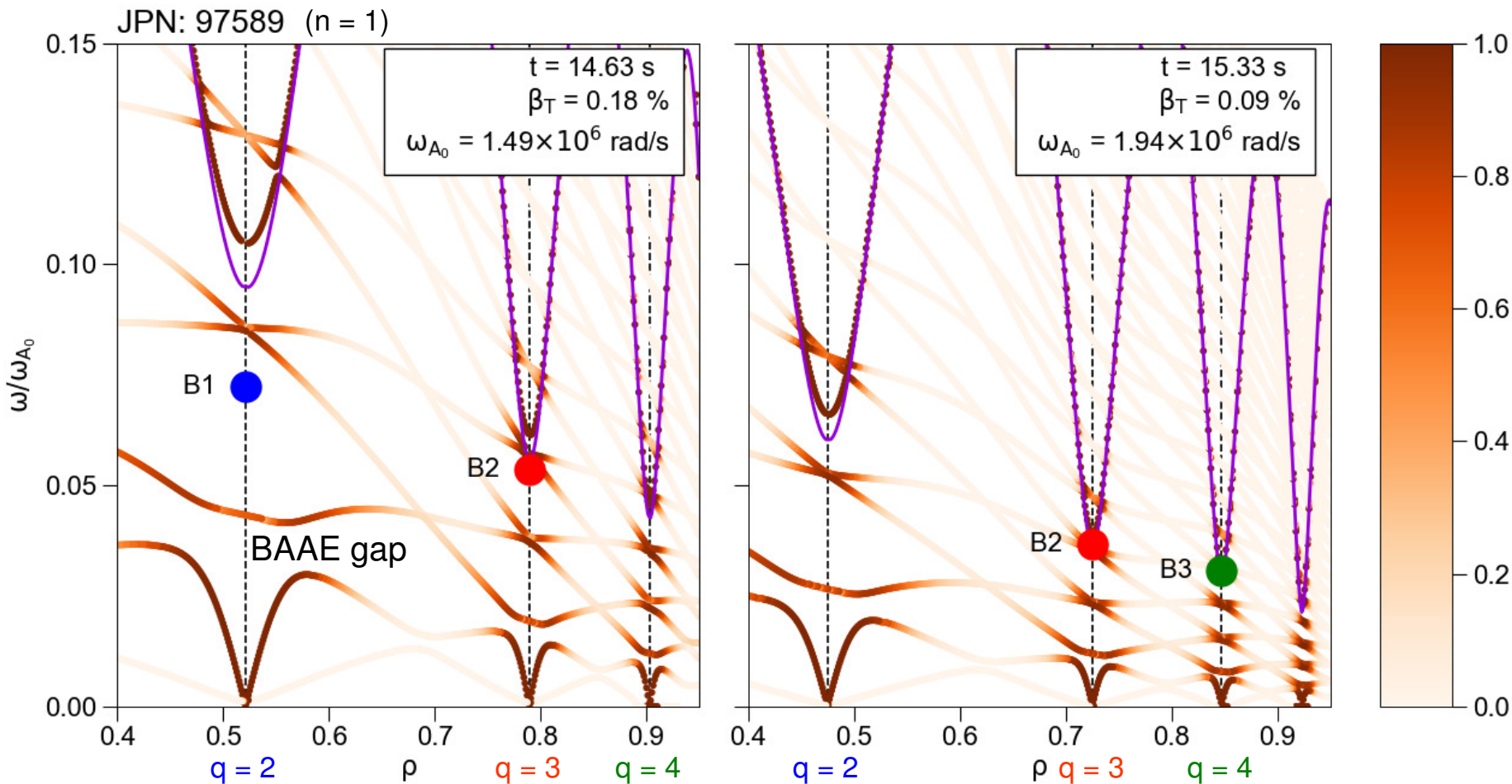
- Opening of **compressibility-induced gaps** in the low-frequency region ($\omega/\omega_A < 0.1$), with the frequencies B1, B2 and B3 located near the minimum values of the dispersion curve at the different resonant surfaces.



SAW-ISW coupled continuum



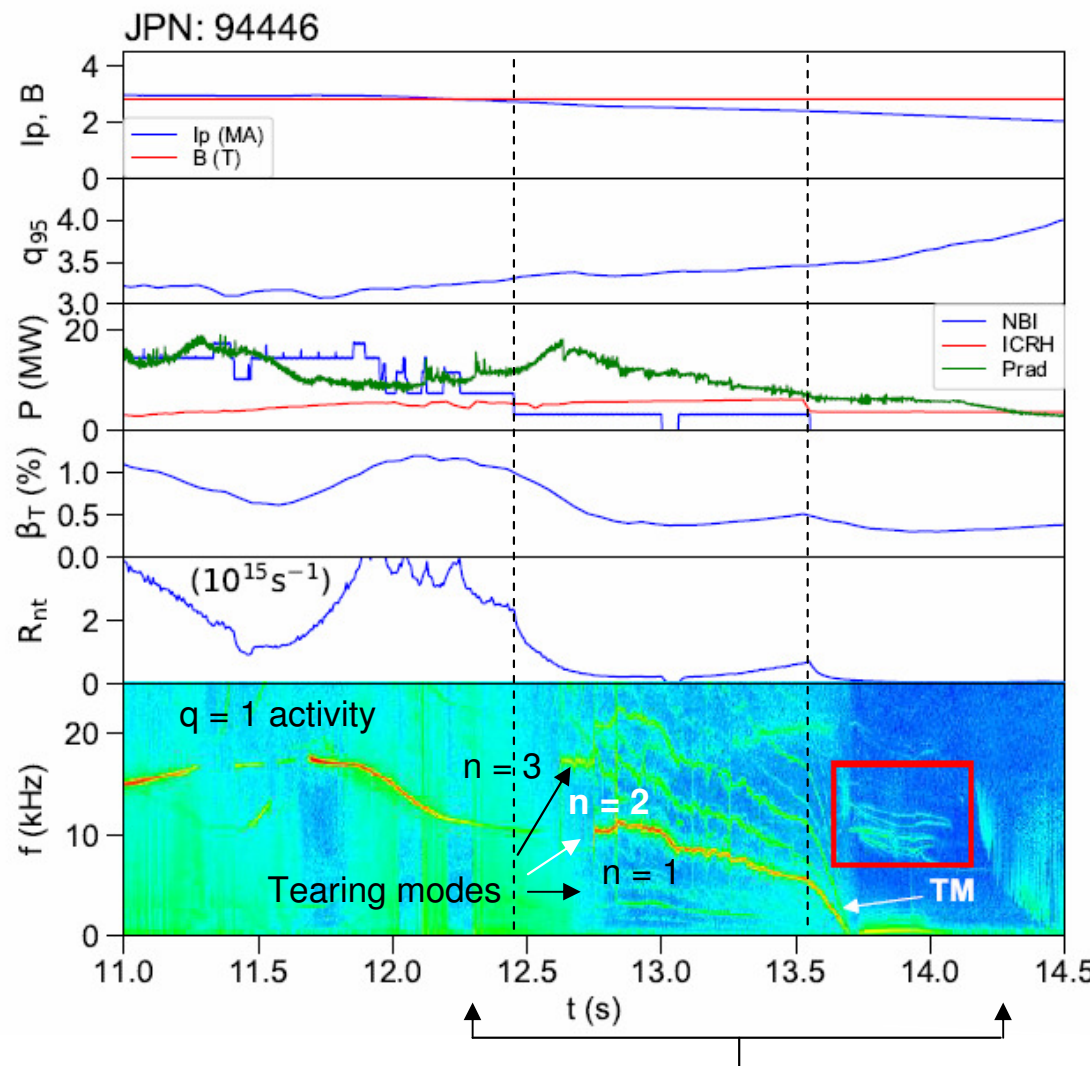
- The so-called “**Alfvénicity**” is introduced as a proxy for mode polarization: 1 for Alfvénic, 0 for acoustic. Good agreement of the fully Alfvénic solution with slow-sound approximation, with frequencies B1, B2 and B3 near the minimum of the fully Alfvénic solution.
- A lower frequency gap ($\omega/\omega_A < 0.05$) can be seen, corresponding to the frequency range of BAAE, with dispersion curves characterized by mixed **Alfvénic-acoustic polarization**: higher mode damping.



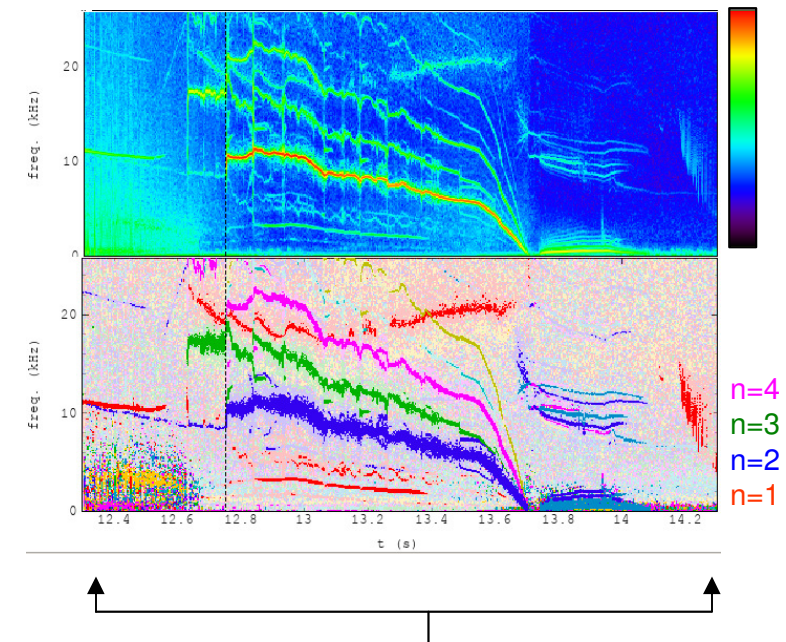
Excitation of BAEs with $n = \pm 2$



- Experimental observation of (multiple) magnetic oscillations with $n = \pm 2$ in the BAE range (5-20 kHz) is reported for the first time in this work.



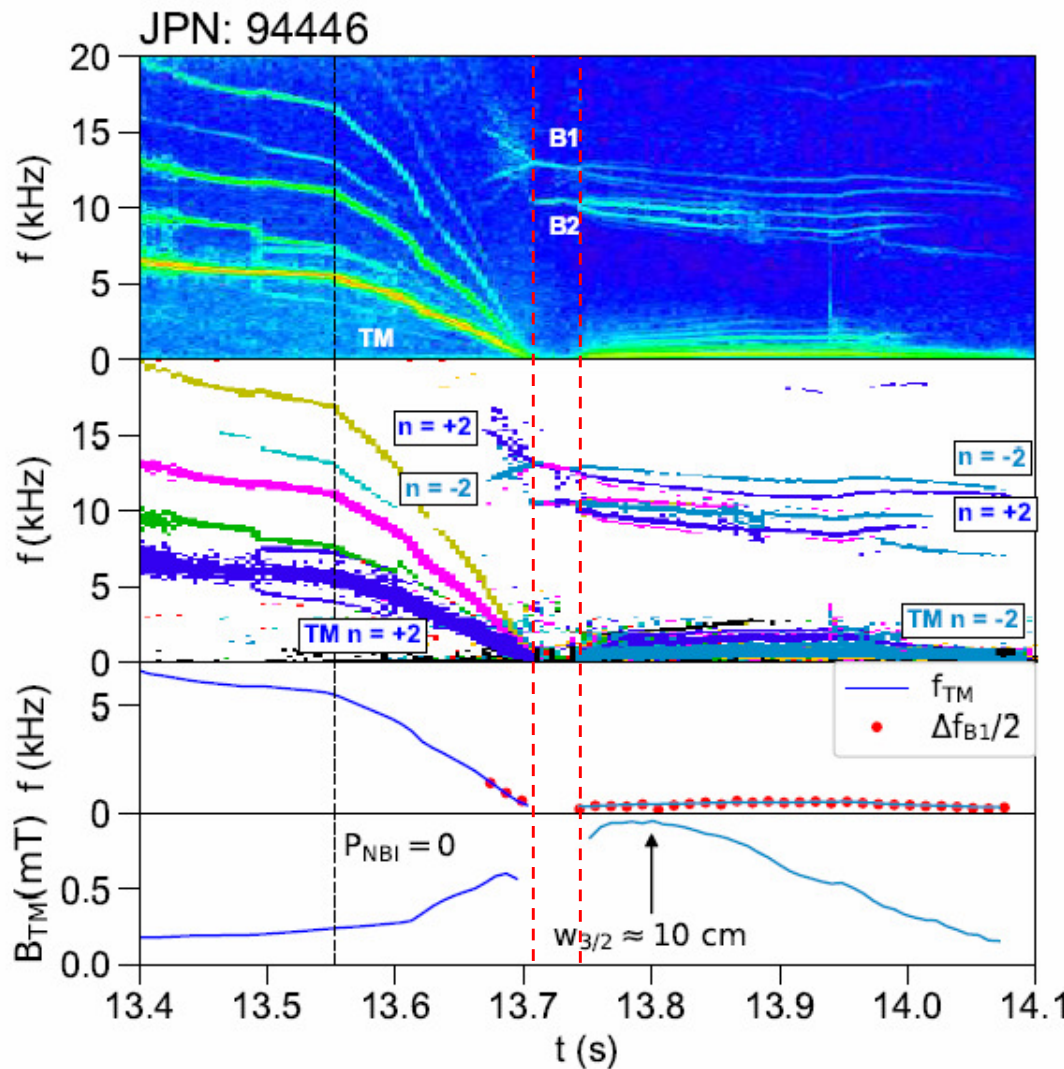
- **NBI power** greatly reduced to 3 MW at 12.4 s and switched-off at 13.6 s.
- **ICRH power** reduced from 6.0 MW to 3.5 MW at 13.6 s.
- Different TMs are observed, the most relevant one in a $n = 2$ TM triggered by a reconnection event at 12.7 s.



Excitation of BAEs with $n = \pm 2$



- Experimental observation of (multiple) magnetic oscillations with $n = \pm 2$ in the BAE range (**5-20 kHz**) is reported for the first time in this work.



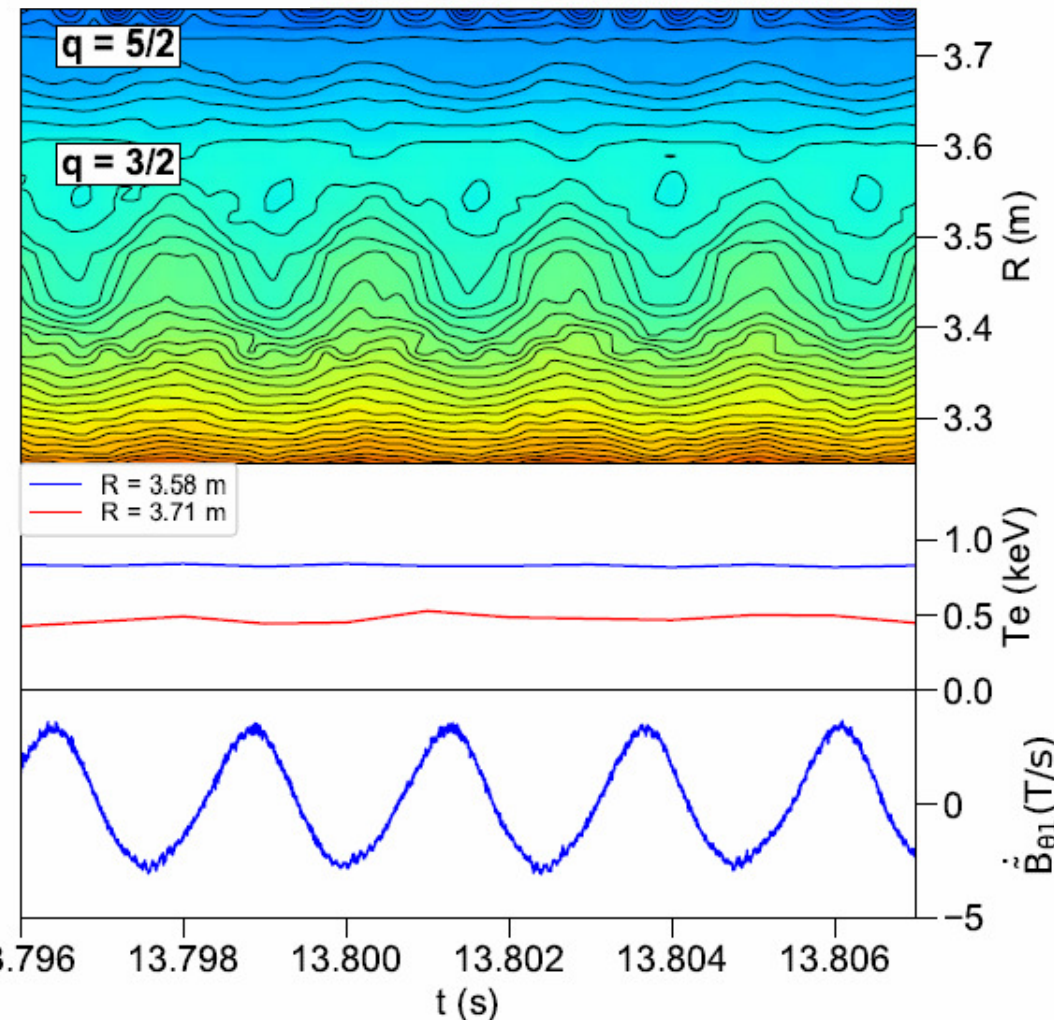
- Frequency values consistent with the **low-frequency beta-induced gap**.
- Oscillations splitted in **two branches** with opposite n : **co-rotation** and **counter-rotation** with TM.
- Frequency difference between branches is twice the TM frequency (**Doppler shift**):
$$f_{B_{Co}, B_{Cn}} = f_B \pm f_{TM}$$
- **Threshold** on tearing mode amplitude for BAE excitation.

Excitation of BAEs with $n = \pm 2$



- Simultaneous presence of magnetic islands on two different resonant surfaces in a pulse with BAE oscillations at two different frequencies, which scale with the plasma temperature at the resonant surfaces.

JPN: 94446

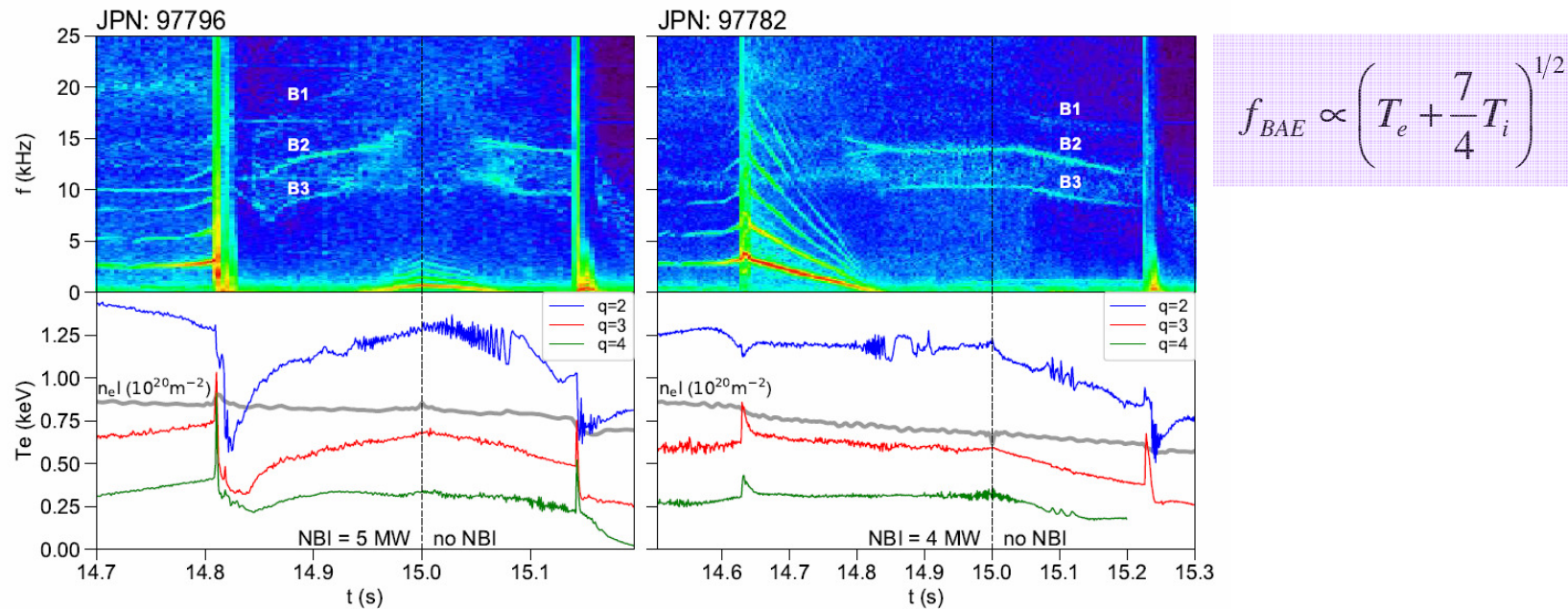


- CAP frequency values from cylindrical equation and from FALCON code:
 $f_{CAP}^{(3/2)} \approx 25 \text{ kHz}$ (20 kHz) ; $f_{B1} \approx 13 \text{ kHz}$
 $f_{CAP}^{(5/2)} \approx 20 \text{ kHz}$ (13 kHz) ; $f_{B2} \approx 10 \text{ kHz}$
- The possibility that the two components B1 and B2 are associated with another pair of islands, i.e. 5/2 and 7/2, cannot be ruled out (q_{95} is changing from 3.4 to 3.7).

Dependencies on plasma parameters: T_e , n_e



- General agreement between the frequency of the components **B1**, **B2** and **B3** and the **electron temperature** on the rational surfaces corresponding to $q = 2$, 3 and 4 , supporting the hypothesis of different BAEs associated with magnetic islands located on different rational surfaces:



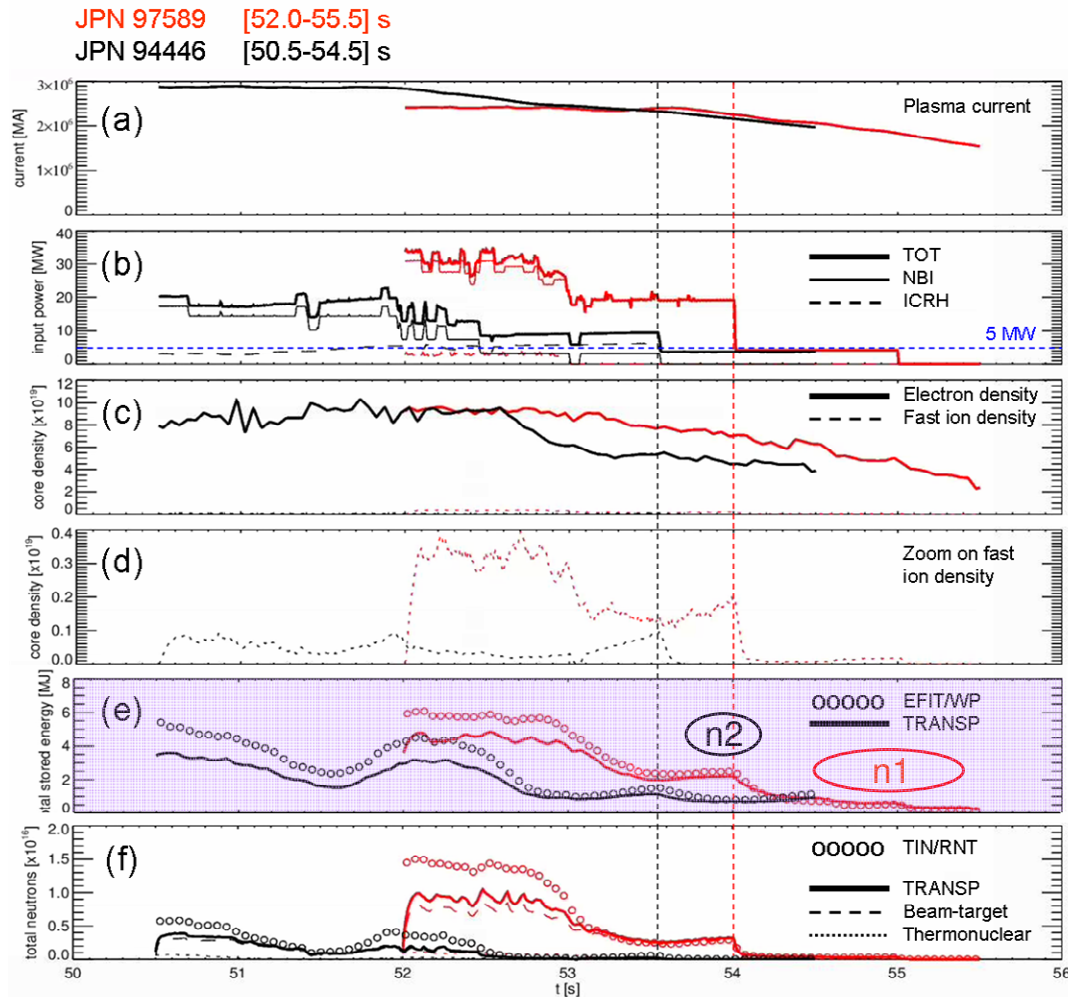
- A sensitivity to **density** is expected for various high-frequency AEs, due to the dispersion relation $\omega \approx k_{\parallel} v_A$ with $k_{\parallel} \propto 1/qR_0$ and $v_A \propto B/\sqrt{n_e}$. However, thermal plasma compression effects play important roles in dispersion relations, so some dependencies are not to be expected.

$$\omega_{BAE} = \omega_0 + \Delta\omega_0 \quad ; \quad \Delta\omega_0 = \frac{\omega_{*n_e}}{2} \left(\frac{\eta_i}{\tau} + \frac{1+\tau}{7/4+\tau} \right) \quad \text{diamagnetic effects}$$

Dependencies on plasma parameters: T_i



- To highlight the dependency on T_i it would be necessary to observe BAE in phases with strongly variable additional heating, changing the ratio T_i/T_e [Xu 2013]. However, the observations of BAEs refer to phases where the total input power (NBI+ICRH) was below 5 MW, so $T_i \approx T_e$ (confidence of about 10%).

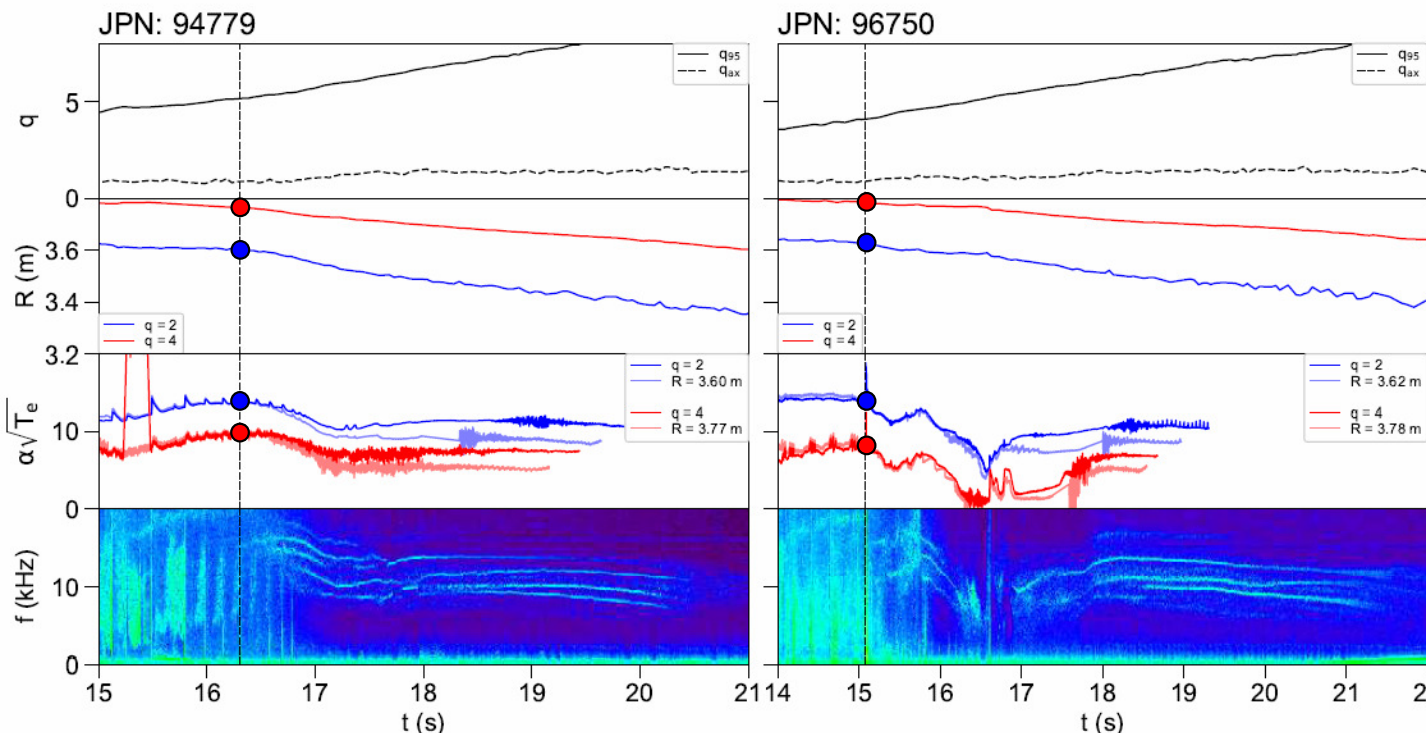


- Measurements of T_i by CXRS available only during the main NBI heating phase ($T_i/T_e \sim 1.3$).
- TRANSP simulations confirm that, assuming $T_i = T_e$, the numerical and experimental stored energy are in good agreement in the time window of interest.
- The fast ion population suddenly drops in about 100 ms ($n_{fi}/n_e \sim 2.5\% \rightarrow 0.2\%$ in JPN 97589), indicating that the fast ions do not have a leading role in BAE excitation.

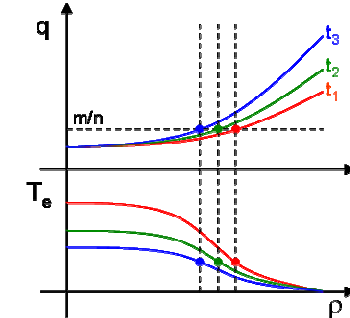
Dependencies on plasma parameters: $q(\rho)$



- A change of $q(\rho)$ can shift the position of the rational surfaces, possibly affecting the BAE frequencies [Xu 2013], which are linked to the temperature at the rational surfaces. The effect is more evident if the variation of $T_e(\rho)$ is small compared with the variation of $q(\rho)$.



- Inward shift of the rational surfaces during the ramp-down (increase in q_{95}).
- T_e variation at fixed radii following the decrease of the heating power.

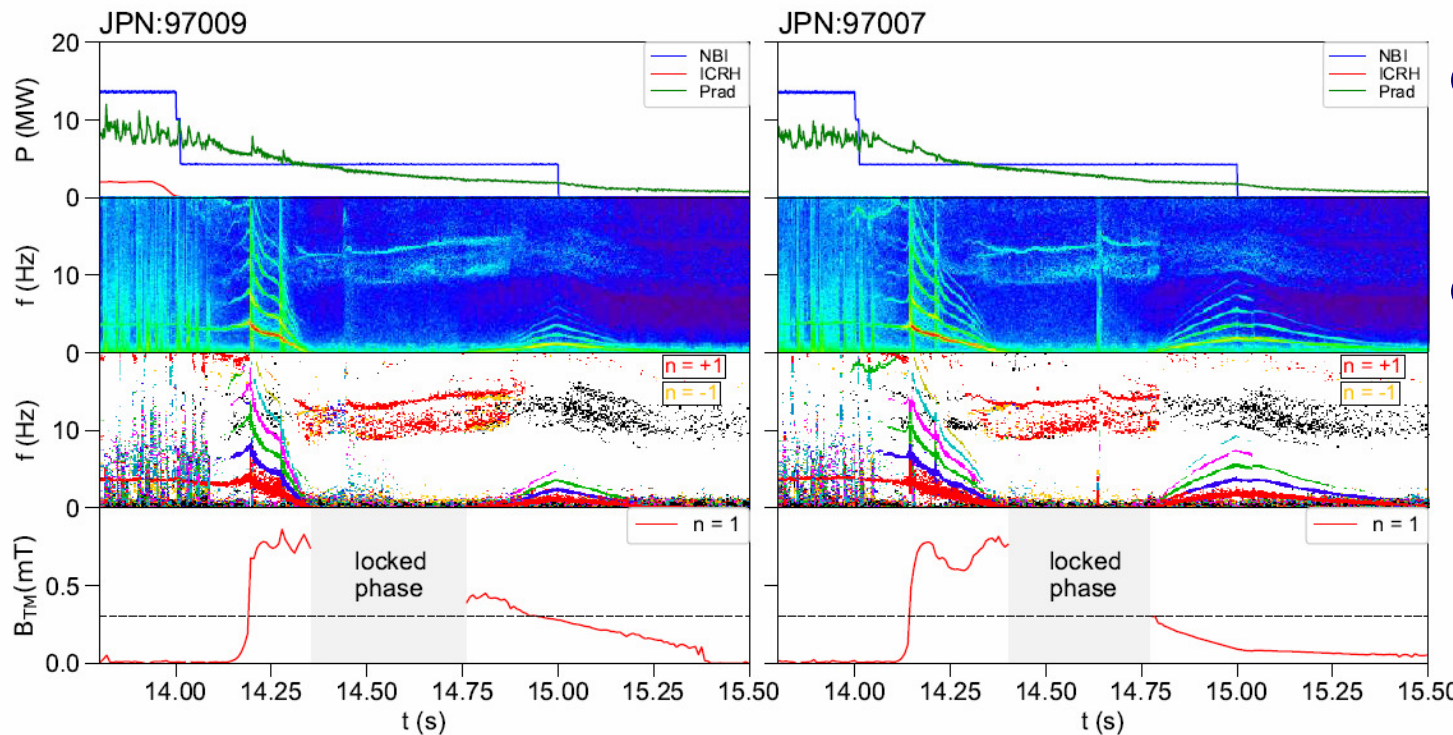


- JPN 94779: the combination of the two effects leads to approximately constant temperature at the rational surfaces (and BAE frequencies).
- JPN 96750: dominant effect of changes in temperature profiles with respect to changes in the position of the rational surfaces (and BAE frequencies).

Threshold on the magnetic island width (n = 1)



- The additional oscillations in the BAE range are observed only for higher values of the TM amplitude, suggesting that the oscillations could tap their energy from the TM by a **non-linear coupling mechanism**. The existence of a critical island width to excite BAE is in agreement with the need to have magnetic islands sufficiently large to transfer enough energy to BAE to **overcome Landau damping**.



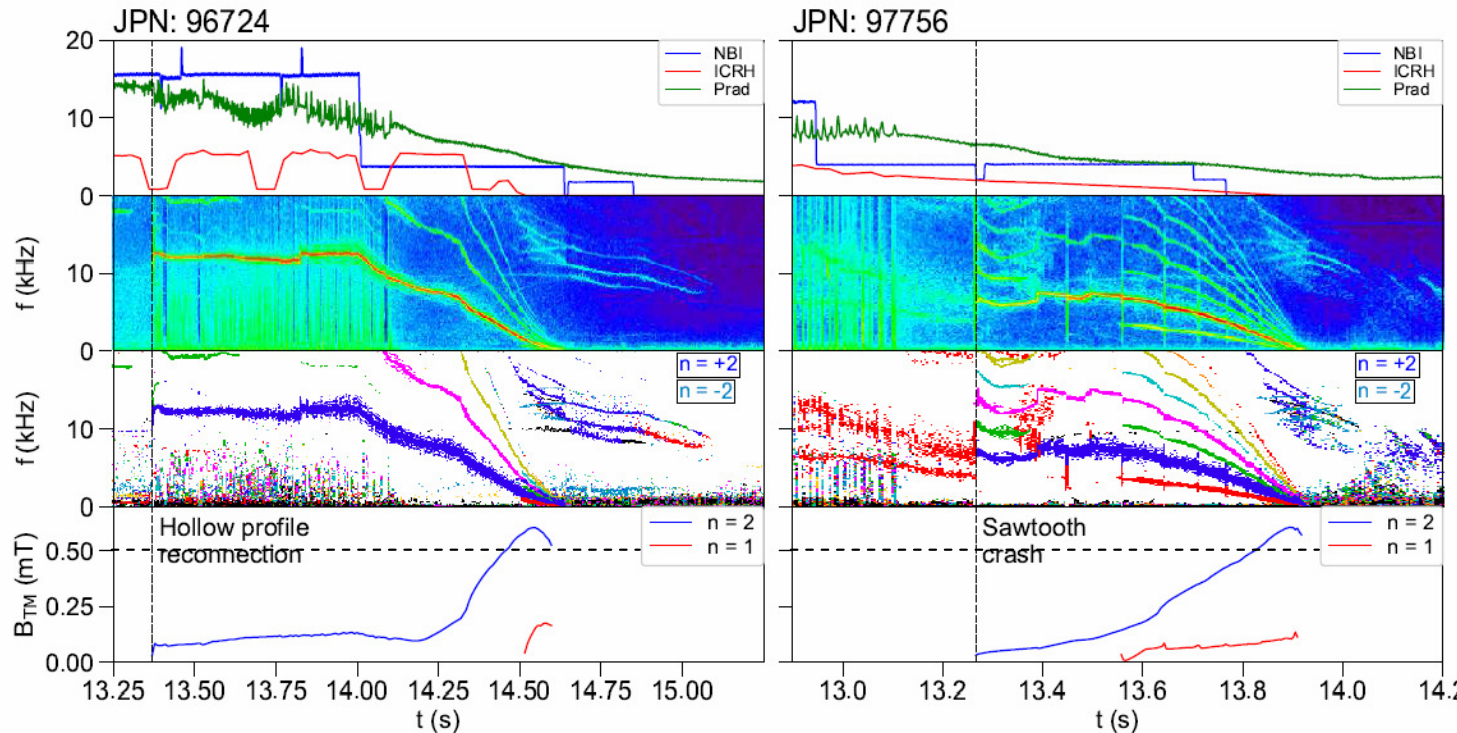
- BAE ($n = \pm 1$) disappear when the TM amplitude reduces below **0.3 mT**.
- Such a threshold could depend on various plasma parameters.

$$w = 4 \sqrt{\frac{R_0 r_s}{n s_s} \frac{B_{r1}(r_s)}{B_T}} \approx 4 \sqrt{\frac{R_0 r_s}{n s_s} \frac{1 - (r_s/r_w)^{2m}}{1 + (r_c/r_w)^{2m}} \left(\frac{r_c}{r_s}\right)^{m+1} \frac{B_{\theta1}(r_c)}{B_T}} \approx 4 \sqrt{\frac{R_0 r_s}{n s_s B_T} \frac{1}{2} \left(\frac{r_c}{r_s}\right)^{m+1}} \cdot \sqrt{B_{\theta1}(r_c)}$$

Threshold on the magnetic island width ($n = 2$)



- The excitation of multiple pairs of $n = \pm 2$ BAE is observed in two pulses with $n = +2$ TM triggered by a reconnection process, when the TM amplitude exceeds **0.5 mT**.



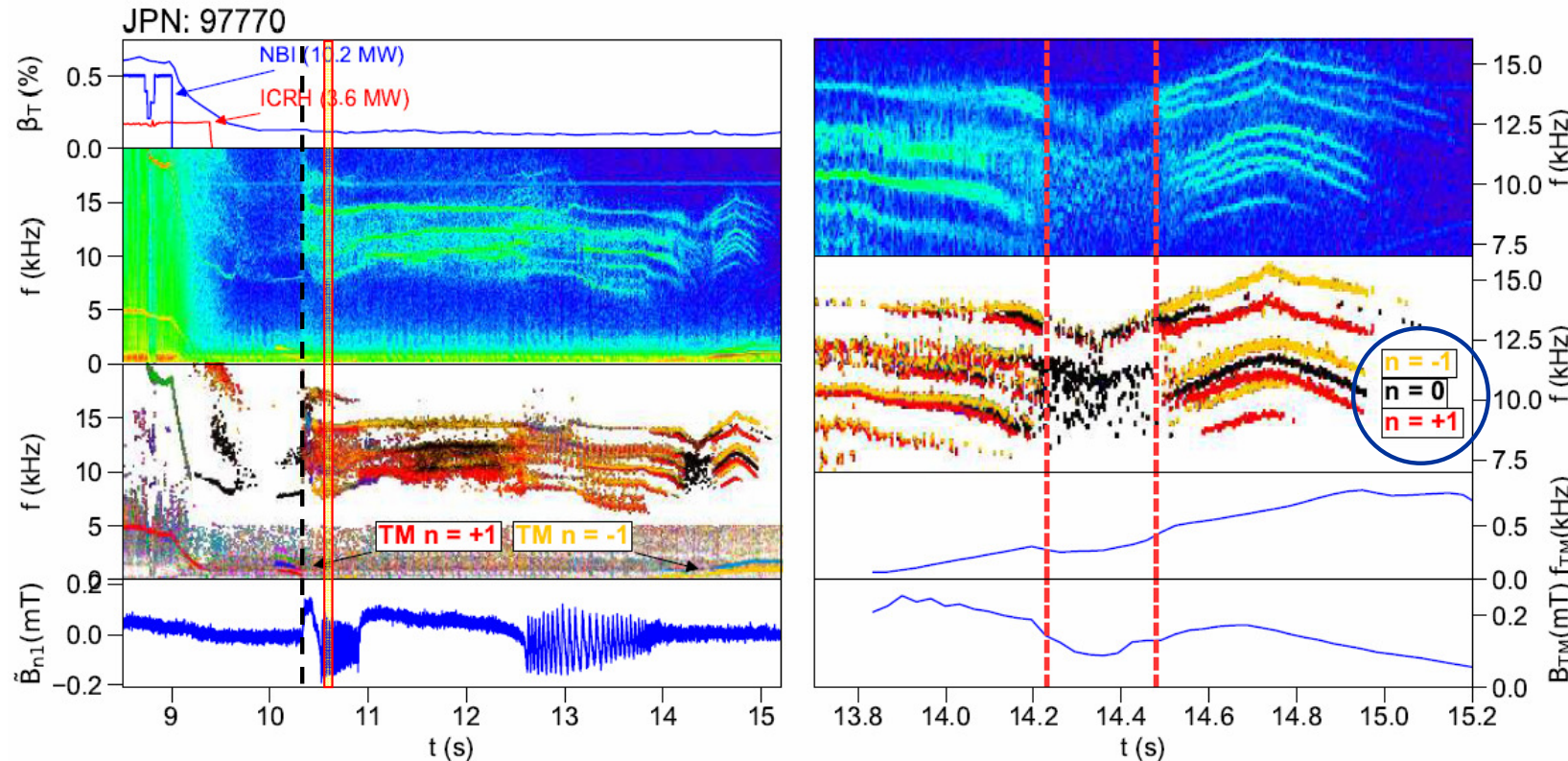
- Trigger for TM onset can be either a reconnection event in hollow Te profiles or a sawtooth crash in peaked Te profiles.

- In these pulses a $n = +1$ TM is also present, without the excitation of the BAEs with the same toroidal mode number, likely due to the low amplitude value (below 0.2 mT), as additional confirmation of the existence of a minimum TM amplitude to excite BAEs.

Non-linear mode coupling in the late landing phase



- Long lasting BAE are sometimes observed between 5 and 20 kHz in the **late landing phase** of JET pulses in the presence of TM, with both NBI and ICRH turned-off and no source for any fast particles.
- Some pulses, characterized by slowly rotating magnetic islands, exhibit additional oscillations with $n = 0$, likely associated with GAM.

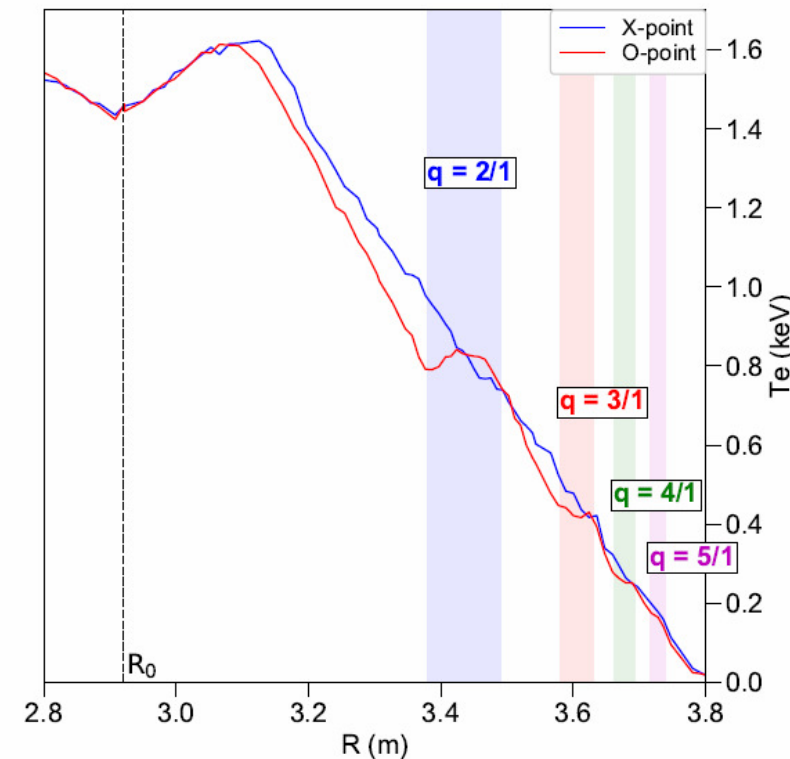
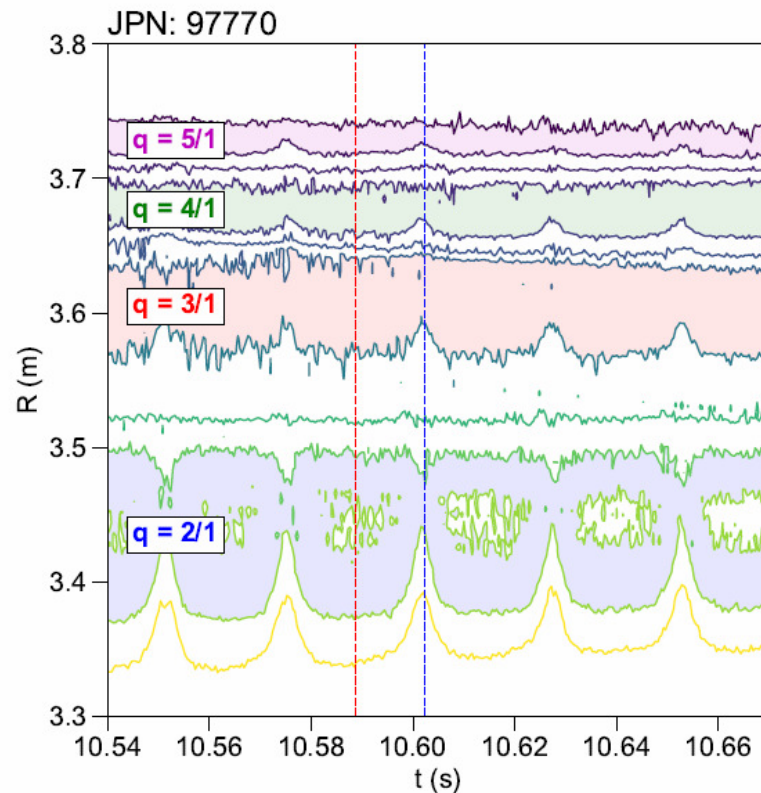


- A **threshold effect** is visible, with more diffuse BAE and GAM signals in correspondence with a decrease of the TM amplitude, reinforcing the hypothesis of the **non-linear interaction** between TM, BAE and GAM [Chen 2013].

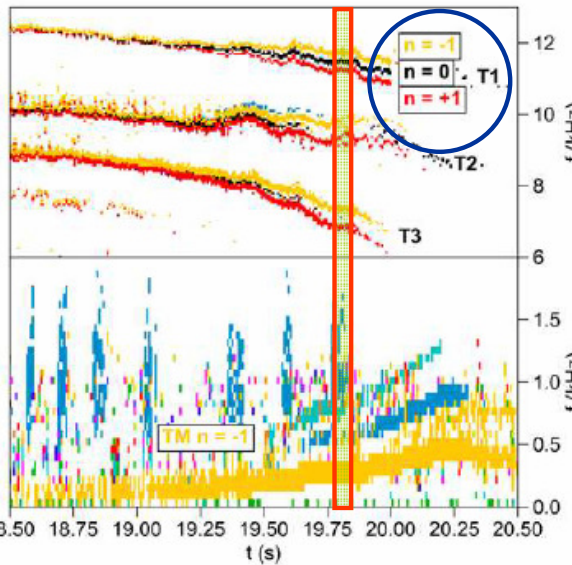
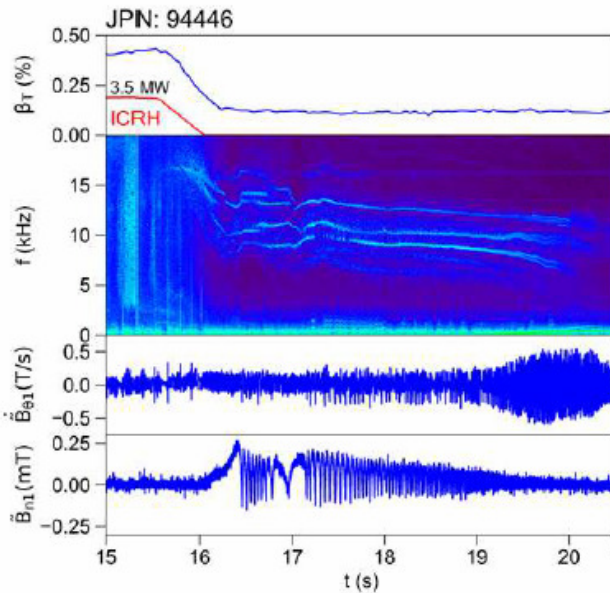
Non-linear mode coupling in the late landing phase



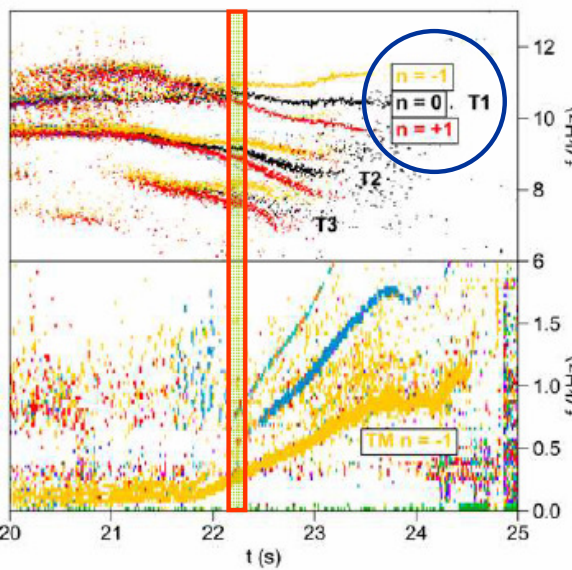
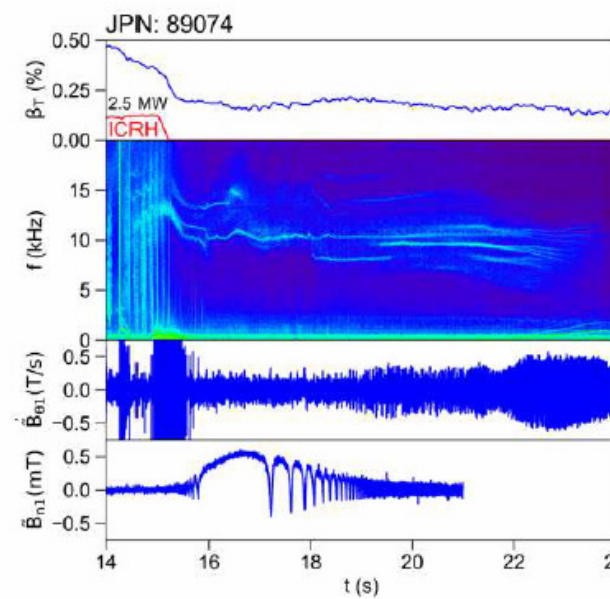
- The hypothesis that BAEs with different frequencies are associated with **magnetic islands on different resonant surfaces** (all rotating with the same toroidal velocity) is supported by the ECE contours and by the flattening regions in the Te profile corresponding to the island O-point.



Multiple “triplets”: “twin BAEs” plus GAM



- Multiple pairs of branches with $n = -1$ and $n = +1$ are observed when a faster TM rotation is recovered, with the two branches separated by two times the TM frequency.



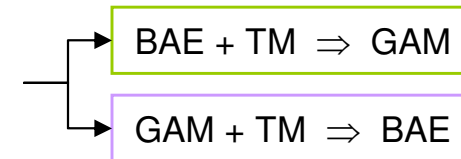
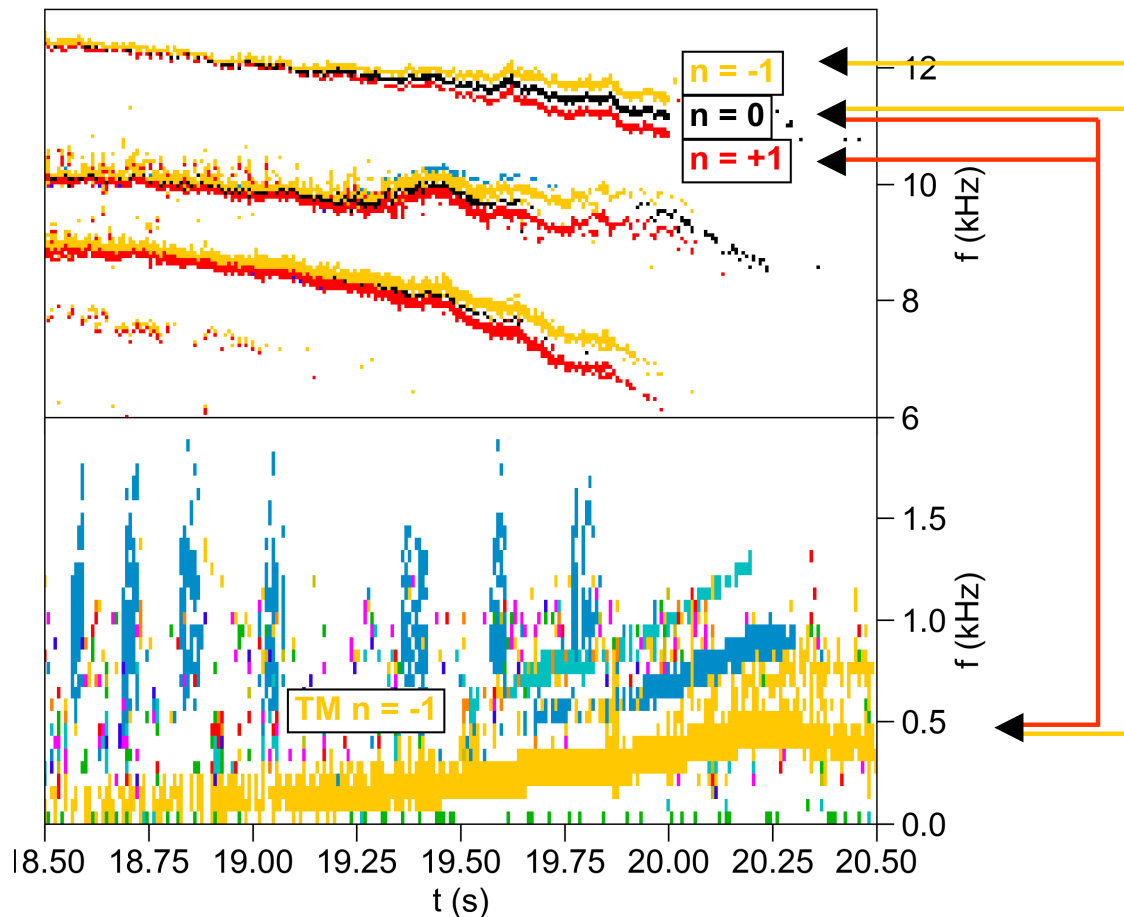
- An $n = 0$ component is detected at the exact middle frequency between each pair of branches.
- The two extreme branches of each “triplet” can be interpreted as “twin BAEs”, and the central one as a GAM.

Non-linear interaction



- Relationship between frequencies and toroidal mode numbers suggest a **non-linear interaction** (i.e., three wave coupling) between the modes (TM, twin BAEs and GAM).
- Two interpretations can be given of such a non-linear interaction:

JPN: 94446



Matching conditions

$$f_{BAE, Co} - f_{TM} = f_{GAM}$$

$$f_{BAE, Cn} + f_{TM} = f_{GAM}$$

$$f_{BAE, Co/Cn} \mp f_{TM} = f_{GAM}$$

(same conditions on n)

The direction of wave energy transfer is unknown

$$f_{GAM} \pm f_{TM} = f_{BAE, Co/Cn}$$

Bicoherence analysis \rightarrow
(no causal effects)

Cross-spectral coherence and bicoherence



- Mathematical definitions used to calculate the coherence and the bicoherence between signals coming from **magnetic pick-up coils** positioned at different toroidal angles:

$$S_{ab}(f) \equiv \langle F_a(f) F_b^*(f) \rangle \quad \text{cross-power spectrum}$$

$$S_{aa}(f) \equiv \langle |F_a(f)|^2 \rangle ; \quad S_{bb}(f) \equiv \langle |F_b(f)|^2 \rangle \quad \text{self-power spectra}$$

$$\gamma_{ab}(f) \equiv \frac{\langle |F_a(f) F_b^*(f)| \rangle^2}{\langle |F_a(f)|^2 \rangle \langle |F_b(f)|^2 \rangle} = \frac{|S_{ab}(f)|^2}{S_{aa}(f) S_{bb}(f)} \quad \text{squared spectral coherence}$$

$$PSD_a(f) = \gamma_{ab}(f) S_{aa}(f) ; \quad PSD_b(f) = \gamma_{ab}(f) S_{bb}(f) \quad \text{power spectral density}$$

$$B_{abc}(f_1, f_2) \equiv \langle F_a(f_1) F_b(f_2) F_c^*(f_1 + f_2) \rangle \quad \text{cross-power bispectrum}$$

$$\beta_{abc}(f_1, f_2) \equiv \frac{\langle |F_a(f_1) F_b(f_2) F_c^*(f_1 + f_2)| \rangle^2}{\langle |F_a(f_1) F_b(f_2)|^2 \rangle \langle |F_c^*(f_1 + f_2)|^2 \rangle} \quad \text{auto-bispectrum if } F_a(f) = F_b(f) = F_c(f)$$

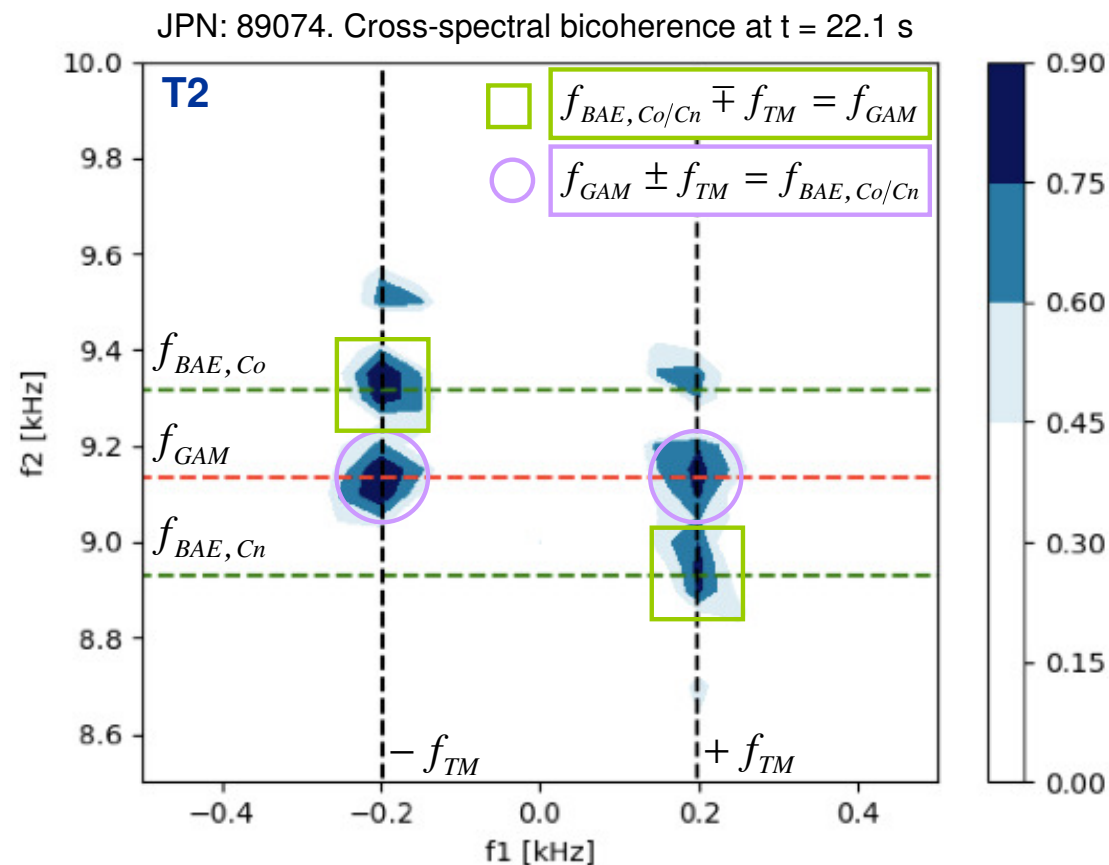
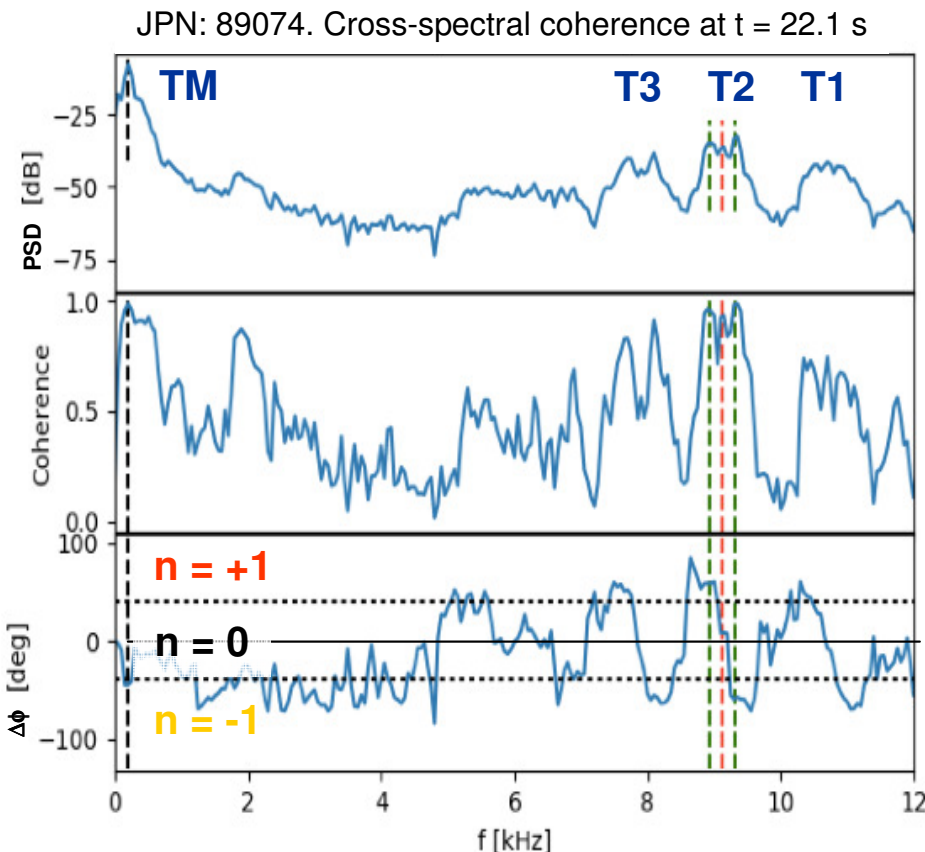
$$\text{squared spectral bicoherence}$$

- Estimate of coherence and bicoherence using **two different signals** ($a = b; c$), with a collection of 40 time windows 20 ms long (overlap is adjusted to cover the whole time interval $\sim 100\text{-}200$ ms).

Cross-spectral coherence and bicoherence



- Cross-spectral coherence and bicoherence analyses of magnetic fluctuations associated with **TM**, **BAE** and **GAM** have been used as indication of a three-wave coupling mechanism, evaluating the degree of phase coherence between the fluctuations of the three modes with two different coils.



- Bicoherence cannot give information on the prevalence of an excitation mechanism on the other one, due to the symmetry of bispectrum. Obtaining additional information on combining electrostatic and magnetic features for GAM [Xu 2021] will be explored in the near future.

Conclusions



- **Multiple oscillations in the BAE frequency range**, with toroidal mode number $n = 1, 2$ have been observed in JET pulses characterized by magnetic islands on different rational surfaces (**first observation ever**), with the values of the BAE frequencies related to the temperatures at the islands' locations.
 - BAE appear in pairs of modes propagating in opposite directions and forming a **standing wave** structure in the island rest frame.
 - The existence of a **critical island width** to excite BAE is in agreement with the need to have magnetic islands sufficiently large to transfer enough energy to BAE to overcome Landau damping.
 - Calculation of the **coupled Alfvén-acoustic continuum** in realistic toroidal geometry by FALCON code, supporting the hypothesis of BAEs rather than BAAEs.
 - Examples of BAE with **$n = +/- 2$** have been reported (**first observation ever**).
- Additional oscillations with **$n = 0$** at the exact middle frequency between each pair of “twin BAEs” observed in pulses characterized by slowly rotating TM in the late landing phase, likely associated with **GAM**.
 - **Non-linear interaction** between TM, BAE and GAM confirmed by cross-spectral bicoherence analysis.
 - Observation of **multiple “triplets”** (twin BAEs plus GAM) due to the simultaneous presence of several magnetic islands in the plasma (**first observation ever**).

Discussion



- The ramp-down phase is not really relevant for possible performance degradation in burning plasmas due to BAEs. However, large magnetic islands can also appear in the flat-top phase of high-performance plasmas and these modes could in principle drive BAEs and GAMs.
- By expanding upon the context of this analysis to steady-state burning plasma devices, BAEs can be as deleterious as TAEs to energetic particle confinement, which is penalizing for plasma heating and harmful for the reactor's first wall, so it is crucial to verify the **agreement between theory and experiment** in present-day tokamak plasmas, in view of ITER and DEMO.
- The BAE/GAM degeneracy is expected to play an important role in the self-organized behaviors of burning plasmas, since their non-linear interplay via zonal structure is expected to be one of the dominant coupling mechanism between the very disparate space-time scales of Alfvénic fluctuations and MHD modes on the one side and plasma turbulence on the other.
- It is important to develop codes dedicated to the calculation of the Alfvén continuum, such as FALCON, and to refine techniques such as the cross-spectral bicoherence analysis to investigate the non-linear interaction between TMs, BAEs and GAMs.